Adipose-derived stem cell sheets combined with β-tricalcium phosphate/collagen-I fiber scaffold improve cell osteogenesis

YANG WANG[1], XIAOJIA SONG[2], RUI LEI[1], NING ZHANG[3], LIANGPING ZHANG[4], WEI XIAO[1], JINGHONG XU[1] and JUN LIN[5]

[1]Department of Plastic Surgery, The First Affiliated Hospital, Zhejiang University School of Medicine, Hangzhou, Zhejiang 310003; [2]Department of Orthodontics, Hangzhou Stomatology Hospital, Hangzhou, Zhejiang 310012; [3]Dental Department, The Second Affiliated Hospital, Zhejiang University School of Medicine, Hangzhou, Zhejiang 310009; [4]Department of Plastic Surgery, The First Hospital of Jiaxing, Jiaxing, Zhejiang 314000; [5]Department of Stomatology, The First Affiliated Hospital, Zhejiang University School of Medicine, Hangzhou, Zhejiang 310003, P.R. China

Received June 20, 2020; Accepted January 22, 2021

DOI: 10.3892/etm.2021.9882

Abstract. Transplantation of cell-based material is a promising approach for the treatment of critical bone defects. However, it is still limited by the lack of suitable scaffold material or abundant seeding cell sources. The present study aimed to establish a novel composite of an adipose-derived stem cell (ADSC) sheet and a synthetic porous β-tricalcium phosphate/collagen-I fiber (β-TCP/COL-I) scaffold to enhance osteogenic activity. ADSCs were isolated from 3-week-old female Sprague Dawley rats and the ADSC sheets were prepared in an osteoinductive medium. The study groups included the ADSC sheets/scaffold, scattered ADSCs/scaffold, ADSC sheet alone and scaffold alone. Scanning electron microscopy and energy-dispersive spectrometry were used to observe cell-scaffold interactions and analyze the relative calcium content on the composites' surface. Alizarin red S staining was used to examine the calcium deposition. ELISA and reverse transcription-quantitative PCR were used to detect the expression levels of alkaline phosphatase (ALP), osteocalcin (OCN) and osteopontin (OPN). The results revealed that ADSCs were able to tightly adhere to the β-TCP/COL-I scaffold with no cytotoxicity. The calcifying nodules reaction was positive on ADSC sheets and gradually increased after osteogenic induction. In addition, the β-TCP/COL-I scaffold combined with ADSC sheets was able to significantly enhance the expression levels of ALP, OCN and OPN and increase the superficial relative calcium content compared to scattered ADSCs/scaffold or the ADSC sheet alone ($P<0.05$). The results indicated that ADSCs possess a strong osteogenic potential, particularly in the cell-sheet form and when compounded with the β-TCP/COL-I scaffold, compared to scattered ADSCs with a β-TCP/COL-I scaffold or an ADSC sheet alone. This novel composite may be a promising candidate for bone engineering.

Correspondence to: Dr Jinghong Xu, Department of Plastic Surgery, The First Affiliated Hospital, Zhejiang University School of Medicine, 79 Qingchun Road, Hangzhou, Zhejiang 310003, P.R. China
E-mail: 1304017@zju.edu.cn

Abbreviations: MSCs, mesenchymal stem cells; ADSCs, adipose-derived stem cells; β-TCP/COL-I, β-tricalcium phosphate/collagen-I fiber; ALP, alkaline phosphatase; OCN, osteocalcin; OPN, osteopontin

Key words: adipose-derived stem cells, β-tricalcium phosphate/collagen-I fiber scaffold, cell sheet, osteogenesis, bone engineering

Introduction

The reconstruction of critical bone defects caused by trauma, excision of tumors or deformity remains a significant challenge in the clinic. Autologous bone tissue grafting has been considered as the gold standard therapeutic strategy. However, this is usually limited by the lack of donor tissues that may be harvested and considerable grafting failure rates (1). In recent years, cell-based bone regenerative therapy using mesenchymal stem cells (MSCs) has become a promising bone reconstruction strategy (2). Adipose-derived stem cells (ADSCs) represent an attractive cell source due to their abundance in the body, and a less invasive and painful harvesting procedure than that for other stem cells (1,3). Furthermore, ADSCs have a self-renewal capacity, high proliferation (4) and a good ability to differentiate into osteogenic lineages (5). These features have made ADSCs a promising candidate for bone tissue engineering.

Since a single-cell suspension lacks cell-to-cell connections, the rates of cell engraftment, survival and proliferation on target tissues are frequently insufficient. Cell sheet technology provides an effective strategy to tackle these challenges (6). The cell sheets possess an abundant extracellular matrix (ECM), which may be used as a natural biological scaffold (7), providing an ambient microenvironment through which resident cells may communicate with each other (8). This also provides a channel for nerves, blood vessels and the diffusion of oxygen and nutrients *in vivo*. In addition, the cell sheets easily attach to the surface of other scaffolds, cell sheets

or host tissues in tissue engineering (9). A previous study suggested that the cell sheets wrapped around the scaffold exhibited a more pronounced bone regeneration ability than cells dispersed in a scaffold (10).

A suitable biomaterial scaffold that accommodates seeding cells is another approach to induce efficient bone regeneration for filling small or large bone defects (11). Various materials have been previously reported to be used for the healing of bone defects (12). However, the optimization of biomaterial scaffolds is still an active research field. Most of the existing scaffolds have several limitations, including mediating inadequate cell migration, proliferation or nutritive transportation to secrete a sufficient ECM, establish cell-to-cell interactions and induce severe inflammatory reactions *in vivo* (13). Collagen (COL) is a major bone component and has excellent biocompatibility with proper interconnected porous structures for cell proliferation (14). Furthermore, β-tricalcium phosphate (β-TCP) has been widely used in bone engineering due to its good osteoconductivity, cellular adhesion, ability to accelerate differentiation and superior biodegradability (15). In the present study, collagen-I fibrils integrated with homogeneous β-TCP particles as units were used to construct a porous β-TCP/COL-I scaffold, simulating the compositional and microstructural characteristics of natural bone. This novel porous scaffold had 95% porosity, a pore diameter of 50-100 μm, no reported cytotoxicity and suitable mechanical properties (14,16). In addition, the porous microstructure facilitates the ingrowth of local cells and delivery of nutrients and oxygen, which are crucial for successful bone regeneration (10,17).

In the present study, a compound of ADSC sheets wrapped around a β-TCP/COL-I scaffold was established. Its advantages in osteoinductivity compared with those of merely ADSC sheets or scattered ADSCs with a β-TCP/COL-I scaffold were investigated *in vitro*. The present study aimed to explore an improved composite of seeded cells and biomaterial, which is expected to become a novel approach for bone regeneration in the future.

Materials and methods

ADSC isolation and cultivation. Female Sprague-Dawley rats (age, 3 weeks; body weight, 70-80 g) were purchased from the Laboratory Animal Center of Zhejiang Province. All experimental animal procedures were approved by the Research Ethics Committee of the First Affiliated Hospital, School of Medicine, Zhejiang University (Hangzhou, China) and 30 rats were permitted in the current study (permit no. 2019-748). The rats were sacrificed by cervical dislocation after anesthesia by intraperitoneal injection of 1% pentobarbital sodium (60 mg/kg). Homologous adipose tissue was obtained from the inguinal fat pad and washed thrice with PBS (Gibco; Thermo Fisher Scientific, Inc.). After being minced into a paste with scissors, the adipose tissue was treated with 0.01 mol/l of type I collagenase (Sigma-Aldrich; Merck KGaA) at 37˚C for 50 min and then neutralized with fetal bovine serum (FBS; Sigma-Aldrich; Merck KGaA). Subsequently, the solution was filtrated using a gauze strainer (75-μm mesh) and centrifuged at 152 x g, 25˚C for 8 min. Afterward, these cells were cultured in Dulbecco's modified Eagle's medium (DMEM), which contained 10% FBS, 100 mg/ml of streptomycin and 100 U/ml of penicillin (all from Gibco; Thermo Fisher Scientific, Inc.), and cultured at 37˚C in an atmosphere with 5% CO_2. The medium was replenished every 2-3 days. When the cultures grew to 70-80% confluence, the cells were washed with PBS, digested with 0.25% trypsin and 0.02% EDTA (Sigma-Aldrich; Merck KGaA) and then sub-cultured.

ADSC sheet preparation and osteogenic differentiation. ADSCs at the 3rd passage were harvested for further experiments. To create the cell sheets, the ADSCs were cultured at a density of $1x10^5$ cells/cm^2 with regular medium in a 6-cm cell culture dish until they reached 70-80% confluence. For osteogenic induction, the regular medium was replaced by the osteoinductive medium, which contained 0.1 M of dexamethasone, 10 mM of β-phospherglycerol and 50 mg/l of ascorbic acid (all from Sigma-Aldrich; Merck KGaA). The medium was subsequently refreshed every 2 to 3 days. After culturing for 10 days, the ADSC sheets were mechanically scraped from the periphery and separated from the culture dish with a scraper and forceps. Three ADSC sheets were fixed with 4% paraformaldehyde and stained with hematoxylin and eosin for histological observation.

Alizarin red S staining. The cell sheets were continued to be cultured with osteoinductive medium for 21 days. On days 0, 5, 10, 15, 18 and 21, the ADSC sheets were subjected to Alizarin red S staining. The cell sheets were rinsed twice with PBS, fixed with 95% ethanol at 4˚C for 15 min and washed thrice with double-distilled water. The cell sheets were then stained with 0.1% Alizarin red S-Tris-Hcl (pH 8.2; Sigma-Aldrich; Merck KGaA) for 30 min at 37˚C, washed with distilled water and observed with a phase-contrast microscope (BX41; Olympus Corp.).

Preparation of the β-TCP/COL-I scaffold. Porous β-TCP/COL-I composite scaffolds were prepared as previously described (10). In brief, calcium chloride, polyethylene glycol (both from Shanghai Chemical) and trisodium phosphate (Nanjing Chemical, China) was used to prepare the β-TCP powder. Type-I collagen (Sigma-Aldrich: Merck KGaA) was disassembled into fibrils in an acid solution. Subsequently, the β-TCP particles were added to the collagen fibril suspension and integrated with the fibrils to form bone-like collagen fibrils. After freeze-drying, the porous β-TCP/COL-I composites were obtained. The microstructure of the β-TCP/COL-I scaffold was examined using a field-emission scanning electron microscope (SEM; FE-SEM SU70; Hitachi, Ltd.). The porosity value of the scaffold was evaluated by Archimedes' principle (14).

Cell proliferation assay. In 96-well plates, 100-μl suspensions of dispersed ADSCs were cultured at the center of the β-TCP/COL-I scaffold at a density of $1x10^5$ cells/cm^2 in DMEM containing 10% FBS. From the 2nd day, ADSCs with/without the β-TCP/COL-I scaffold were serum-starved for 48 h in DMEM, which contained 1% FBS. On the 4th day, the medium was replaced by DMEM containing 10% FBS and cells were able to re-enter the cell cycle. After 24 h of culture, the cell proliferation was determined with an MTT

assay (Sigma-Aldrich; Merck KGaA). At the time-points of 1, 3, 5, 7 and 9 h, 20 μl MTT solution (5 mg/ml) was added to each well, followed by incubation for 4 h at 37˚C. Next, 150 μl dimethyl sulfoxide was added to each well, followed by gentle agitation for 10 min. The optical density of each well was then measured at 450 nm using a spectrophotometer (Infinite M200; Tecan). The cell proliferation curve was plotted according to the absorbance values.

Preparation of the composite material. The ADSC sheets were wrapped around the β-TCP/COL-I scaffold cylinders (2.0 cm in diameter and 2.5 mm in thickness). Sheets with or without a scaffold were cultured in osteogenic medium to facilitate the re-attachment of ADSC sheets to the surface of the scaffold or culture dish, respectively. The dispersed ADSCs were cultured under the same laboratory conditions and seeded on the β-TCP/COL-I scaffolds for comparison with the sheet protocol and further characterization of cell scaffold interactions. The β-TCP/COL-I scaffold combined with scattered ADSCs was fixed with 2.5% glutaraldehyde (Shanghai Pharmaceuticals) for 2 h, followed by serial dehydration for 15 min in a gradient of ethanol (30, 50, 70, 85, 90 and 100%). Finally, the specimens were air-dried for 60 min and gold-sputtered for 60 sec at 10 A (E-1010; Hitachi, Ltd.). The cell morphology was observed using SEM. After osteogenic induction for 13 days, the β-TCP/COL-I scaffolds with ADSC sheet and the β-TCP/COL-I scaffolds with scattered ADSCs were observed again using SEM according to the above-mentioned procedures and the relative calcium content on the surface of the composites was analyzed by energy-dispersive spectrometry (EDS; FE-SEM SU70; Hitachi, Ltd.).

Experimental groups. Overall, four experimental groups were established: Group 1, an ADSC sheet was wrapped around a β-TCP/COL-I scaffold cylinder and continued to be cultured in osteogenic medium as described above; Group 2, an ADSC sheet was digested with 0.25% trypsin and 0.02% EDTA into scattered ADSCs and then cultured on the surface of a β-TCP/COL-I scaffold in osteogenic medium; Group 3, an ADSC sheet alone without any β-TCP/COL-I scaffold was continued to be cultured in osteogenic medium; Group 4, the β-TCP/COL-I scaffold alone was immersed in osteogenic medium as a blank control. The four groups were continued to be cultured at 37˚C with 5% CO_2 for 13 days.

ELISA of bone differentiation markers and alkaline phosphatase (ALP) activity measurement. The activity of ALP is considered as the major bone regeneration biomarker during the early stages of osteogenesis. Osteocalcin (OCN) and osteopontin (OPN) are two major noncollagenous matrix proteins involved in bone matrix synthesis during the pre-osteoblastic cell stages. ALP, OCN and OPN were evaluated for the evaluation of osteogenic differentiation. Each group was cultured in osteogenic medium and the medium was replenished every 48 h on days 3, 5, 7, 9, 11 and 13. At the indicated time-points, 2 ml of osteoinductive medium from each group was collected and the amount of OCN and OPN released into the medium over the 48 h was examined using an OCN (Rat) ELISA kit (cat. no. E4764; BioVision. Inc.) and a Rat OPN ELISA kit (cat. no. ERA46RB; Thermo Fisher Scientific, Inc.) respectively, according to the manufacturers' protocols. Subsequently, the cell sheets or scattered ADSCs were washed twice in PBS and precooled on ice. After freezing-melting twice with 600 μl of 0.05% Triton X-100 (Sigma-Aldrich; Merck KGaA), the mixed sample was centrifuged at 21,130 x g for 15 min at 4˚C. The supernatant was then collected for measuring ALP activity with an ALP Assay kit (cat. no. 291-58601; Wako LabAssay). The results were normalized relative to the amount of total protein measured by the BCA Protein Assay kit (cat. no. 23227; Thermo Fisher Scientific, Inc.).

Reverse transcription-quantitative PCR (RT-qPCR) analysis. At the indicated time-point, the relative mRNA expressions of ALP, OCN and OPN in Group 1, Group 2 and Group 3 were measured using RT-qPCR. Total RNA was extracted using RNAiso plus (Takara Biotechnology, Inc.) according to the manufacturer's protocol. After quantification by optical density measurement (NanoDrop 2000; Thermo Fisher Scientific, Inc.), 1 μg total RNA was reverse-transcribed into random-primed complementary DNA (cDNA) using a PrimeScript™ RT reagent kit (Takara Biotechnology, Inc.). The PCR reaction system was then prepared according to the manufacturer's protocols of SYBR® Premix Ex Taq™ (cat. no. RR420A; Takara Bio, Inc.) and amplified through real-time PCR using a CFX96 real-time PCR detection system (Bio-Rad Laboratories, Inc.) under the following conditions: 2 min of denaturation at 95˚C, 40 rounds of 10 sec of annealing at 95˚C and 30 sec of extension at 60˚C. The expression levels of the target genes were normalized relative to the housekeeping gene GAPDH. The primer sequences were as follows: GAPDH, 5'-TGTGTCCGTCGTGGATCTGA-3' and 5'-TTGCTGTTGAAGTCGCAGGAG-3'; ALP, 5'-ATGGCTCACCTGCTTCACG-3' and 5'-TCAGAACAGGGTGCGTAGG-3'; OCN, 5'-GACCCTCTCTCTGCTCACTCT-3' and 5'-GACCTTACTGCCCTCCTGCTTG-3'; OPN, 5'-TATCCCGATGCCACAGATGA-3' and 5'-TGAAACTCGTGGCTCTGATG-3'. The results were evaluated using the $2^{-\Delta\Delta Cq}$ method (2,10).

Statistical analysis. The MTT assay was analyzed in three walls and the independent experiments were performed in triplicate (n=3). The data of the MTT assay and the ALP, OCN and OPN levels in each group were expressed as the mean ± standard deviation. All of the data were normally distributed (according to the Kolmogorov-Smirnov-Lilliefors test) and evaluated by parametrical tests (one-way analysis of variance with Scheffe's post-hoc test) using SPSS 19.0 (IBM Corp.). $P<0.05$ was considered to indicate statistical significance.

Results

Characterization of ADSCs and the ADSC sheet. ADSCs exist as polygonal or long spindle-shaped cells in primary culture (Fig. 1A) and they became more homogeneous after the third passage (Fig. 1B). When cultured in osteogenic medium, the ADSCs rapidly proliferated and formed a cell sheet in 10-14 days, and the sheet was easily lifted with a scraper (Fig. 2A). The cell sheet was composed of multiple layers of ADSCs with rich ECM wrapping these cells (Fig. 2B) and the arrangement of the ADSCs changed into a swirling or radial-shape (Fig. 2C). The calcium nodules stained with

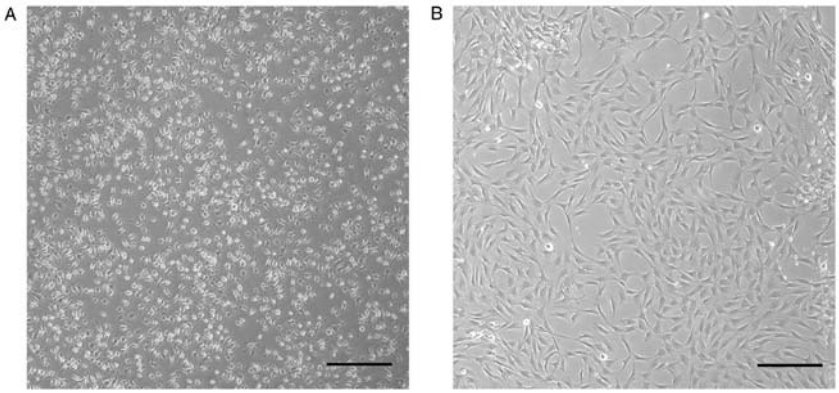

Figure 1. Morphology of adipose-derived stem cells at (A) P0 and (B) P3 under an inverted microscope (scale bar, 100 μm). P, passage.

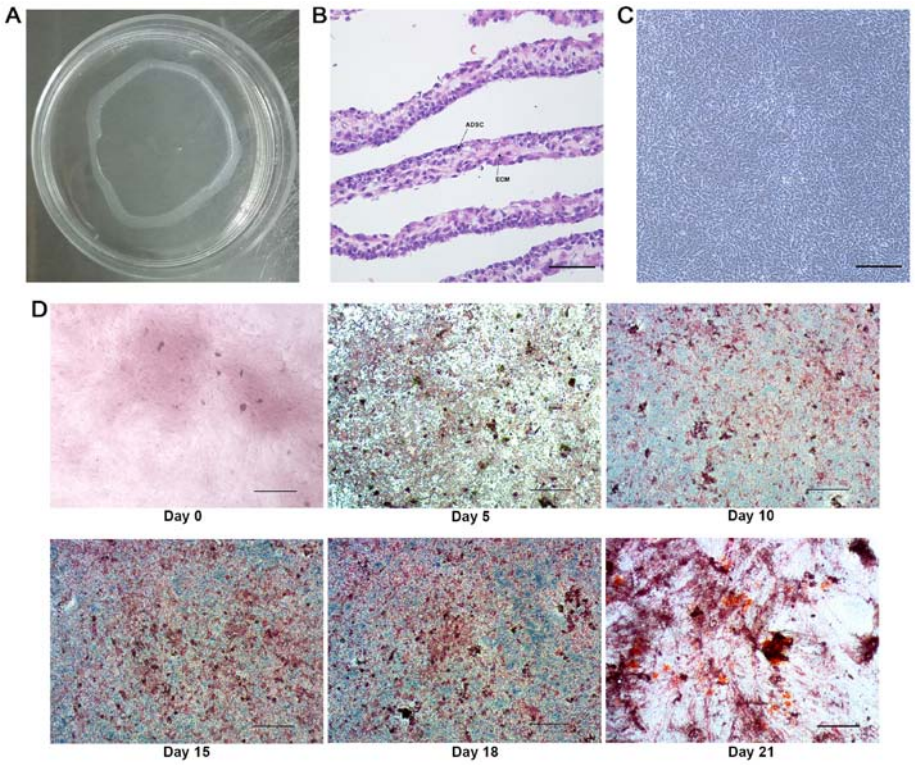

Figure 2. Characterization of the ADSC sheet. (A) Macroscopic appearance of the ADSC sheet harvested using a cell scraper. (B) H&E histological staining of the ADSC sheet, indicating multiple layers of cells with a rich ECM (scale bar, 25 μm). (C) The appearance of the ADSC sheet was observed using an inverted microscope (scale bar, 100 μm). (D) Alizarin red S staining of the ADSC sheet after osteogenic induction on days 0, 5, 10, 15, 18 and 21 (scale bar, 100 μm). ADSC, adipose-derived stem cell; ECM, extracellular matrix.

Alizarin Red S in the ADSC sheet were almost absent on day 0 prior to osteogenic induction and then gradually increased from days 5 to 21 (Fig. 2D), indicating that osteoblastic differentiation was successful.

Characterization of the β-TCP/COL-I scaffold and cell activity of ADSCs on the scaffold. SEM revealed that the β-TCP/COL-I scaffold contained a 3D porous structure with high porosity (~95%) and appropriate pore size (nearly 100 μm) (Fig. 3A). The ADSCs became firmly attached to the surface of the β-TCP/COL-I scaffold and infiltrated into the interconnected pores of the scaffold. They were connected with each other through numerous cellular junctions (Fig. 3B). The MTT assay revealed that the cell proliferation curve of ADSCs on the β-TCP/COL-I scaffold was similar to that of the conventional culture plates and no significant difference was obtained between the two groups at any of the time-points assessed (P>0.05; Fig. 3C), indicating that the scaffold has no cytotoxicity on ADSCs.

Osteogenic differentiation of the ADSC sheet on the scaffold. The bone regeneration biomarkers of osteogenic differentiation in each group were evaluated after osteogenic induction for 3, 5, 7, 9, 11 and 13 days. The relative ALP activity and protein expression levels of OCN and OPN in Group 1 (ADSC sheet combined with a β-TCP/COL-I scaffold), Group 2 (scattered ADSCs combined with a β-TCP/COL-I scaffold) and Group 3 (ADSC sheet alone without a β-TCP/COL-I scaffold)

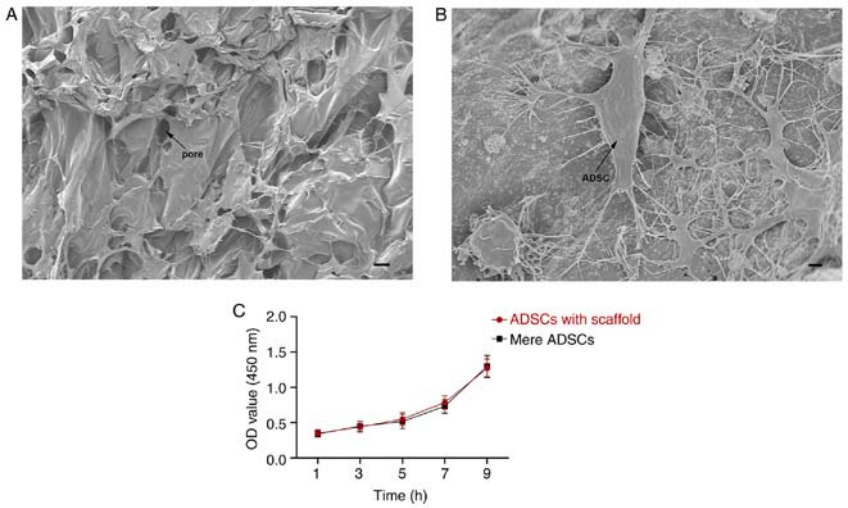

Figure 3. Characterization of the β-TCP/COL-I scaffold. (A) The 3D porous structure of the lyophilized β-TCP/COL-I scaffold was observed by scanning electron microscopy (scale bar, 100 μm). (B) ADSCs adhered to the surface of the scaffold after one day of culture (scale bar, 2 μm). (C) The cell proliferation curve of ADSCs with a scaffold, compared with ADSCs only, evaluated by an MTT assay. OD, optical density; ADSC, adipose-derived stem cell; β-TCP/COL-I, β-tricalcium phosphate/collagen fiber.

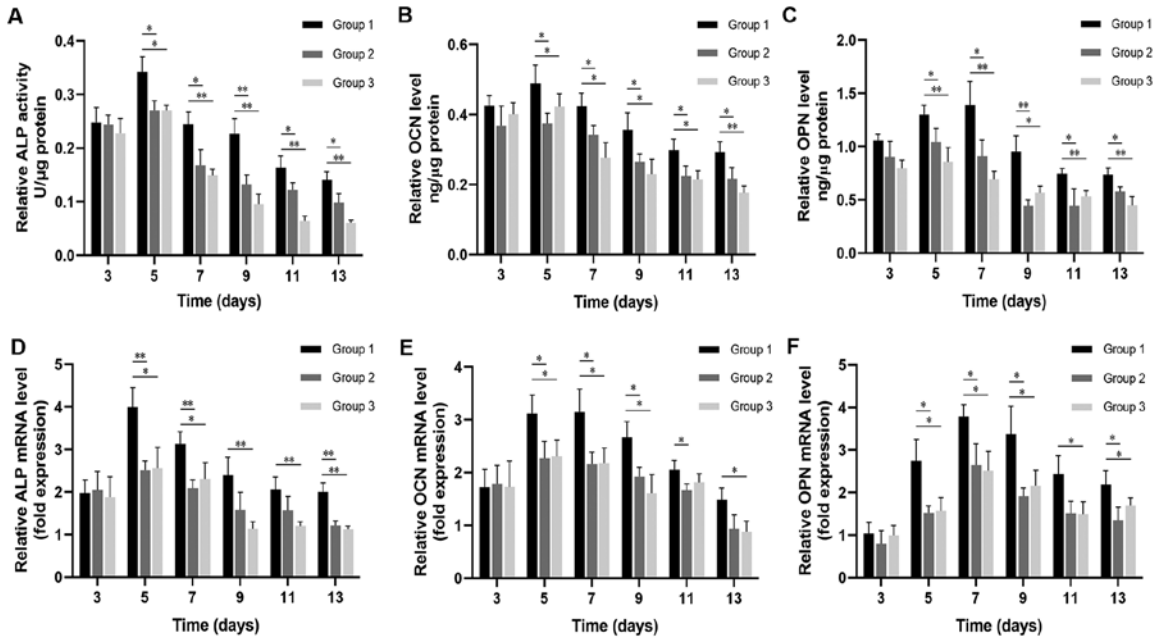

Figure 4. Evaluation of the osteogenic differentiation of the ADSC cell sheet combined with a β-TCP/COL-I scaffold (Group 1), scattered ADSCs combined with a β-TCP/COL-I scaffold (Group 2) and the ADSC cell sheet without a β-TCP/COL-I scaffold (Group 3). Relative (A) ALP activity and protein levels of (B) OCN and (C) OPN. Relative mRNA levels of (D) ALP, (E) OCN and (F) OPN. Values are expressed as the mean ± standard deviation (n=3). *P<0.05; **P<0.01. ADSC, adipose-derived stem cell; β-TCP/COL-I, β-tricalcium phosphate/collagen fiber; ALP, alkaline phosphatase; OCN, osteocalcin; OPN, osteopontin.

reached a peak on day 5 or 7 and exhibited decreases thereafter (Fig. 4). There were no significant differences in these values among the three groups at day 3 (P>0.05). From the 5th day onwards, the protein levels of ALP, OCN and OPN in Group 1 were significantly higher than those in the other two groups (P<0.05 vs. Groups 2 and 3; Fig. 4A-C).

The relative mRNA levels of ALP, OCN and OPN also demonstrated a similar trend. At all the indicated time-points, except for the 3rd day, Group 1 persistently exhibited higher levels of osteogenic mRNA expression than Groups 2 and 3 (P<0.05; Fig. 4D-F). Overall, the ADSC sheet combined with a β-TCP/COL-I scaffold in Group 1 displayed significantly improved osteogenic activity compared to the other two groups.

Calcium content on the scaffold with ADSC sheet. After osteogenic induction for 13 days, the β-TCP/COL-I scaffold with ADSC sheet (Group 1) contained more densely populated cells and mineralized nodules than the β-TCP/COL-I scaffold with scattered ADSCs (Group 2) (Fig. 5A and B, respectively). Furthermore, the relative calcium content of Group 1 was much higher than that of Group 2 as determined by EDS (P<0.05 vs. Group 2; Fig. 5C).

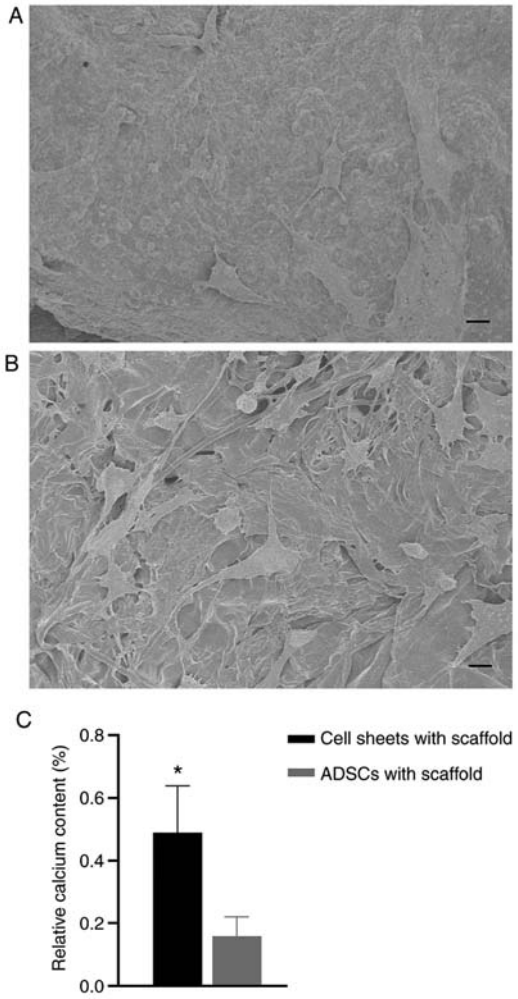

Figure 5. Surface morphologies of two types of complexes visualized by scanning electron microscopy after osteogenic induction for 13 days. (A) β-TCP/COL-I scaffolds with ADSCs sheet (scale bar, 10 μm). (B) β-TCP/COL-I scaffolds with scattered ADSCs (scale bar, 10 μm). (C) Relative calcium content on the surface of the two composites. *P<0.05 vs. ADSCs with scaffold. ADSC, adipose-derived stem cell; β-TCP/COL-I, β-tricalcium phosphate/collagen fiber.

Discussion

Millions of patients suffer from critical bone defects and impaired bone healing, the adequate treatment of which has remained a longstanding clinical problem worldwide (18). Bone tissue engineering as a substitute to autogenous bone grafting brought substantial success in tackling the challenge of repairing bone defects and the use of biomaterials functionalized with bioactive agents to improve bone regeneration in osteonecrosis was considered one of the most promising strategies (12). Available seeding cell sources and suitable biomaterials are currently still being explored and improved (19). In the present study, ADSCs/ADSC sheets and β-TCP/COL-I scaffold composites were established under osteoinductive conditions, in which the ascorbic acid promoted collagen synthesis, the dexamethasone stimulated both osteogenic differentiation and the glycerol phosphate induced mineral deposition. SEM and EDS were used to observe and evaluate the structure of the β-TCP/COL-I scaffold with ADSCs and detect the relative calcium content on the surface of the composites. Histological examination, ELISA and RT-qPCR measurements were used to compare the osteogenic activity of each group. ALP, OCN and OPN are major biomarkers of the early stages of osteogenesis, while calcium deposition is considered a later marker (20). The present results demonstrated that ADSC sheets avoided the cell loss caused by trypsin digestion and had a superior osteogenic performance after being wrapped around a β-TCP/COL-I scaffold when compared to scattered ADSCs with a β-TCP/COL-I scaffold or an ADSC sheet alone. The major advantages of the method of the present study compared with those of previous studies in terms of bone tissue engineering were as follows. First, the ADSCs are easily accessible, abundant and more efficient in osteoinductivity than other MSCs. Furthermore, the ADSC sheets may be harvested using a scraper without enzymatic digestion, which preserved the ECM and cell-cell connections. In addition, the β-TCP/COL-I scaffold had superior biodegradability, osteoconductivity and higher compatibility with ADSC sheets. The composite of ADSC sheets/β-TCP/COL-I scaffold provides a novel promising candidate for bone regeneration.

In bone tissue engineering, promising seeding cells for clinical application must be suitable for isolation and exhibit proliferation efficiency, biocompatibility and formidable osteogenic capacity (21). In a previous study by our group, bone marrow-derived MSCs (BMSCs) were used to construct a stem cell sheet, which had a high bone regeneration potential when combined with β-TCP/COL-I scaffolds (10). In clinical practice, successful repair of huge bone defects via tissue engineering requires a significant number of BMSCs. However, the quantity of autologous BMSCs in the body is limited and the extraction process is frequently painful (21). In addition, long-term *in vitro* culture of BMSCs may compromise their genomic stability (22). Adipose tissues have been considered as a practical and adequate source of stromal precursor cells with a high potential for bone-tissue reconstruction. Compared with BMSCs, ADSCs possess a higher proliferation and self-renewal capacity (3), and a high quantity of ADSCs may be easily obtained from the host. In addition, ADSCs have been proven to possess high efficiency in bone regeneration, in addition to secreting anti-inflammatory factors and decreasing pro-inflammatory responses (23). Furthermore, the differentiation capacity of ADSCs was maintained with aging, thus having advantages over BMSCs (4). The present study revealed that ADSCs, alone or combined with a scaffold, expressed osteogenic biomarkers much earlier than BMSCs in the previous study by our group under the same conditions (10).

Since the traditional method of seeding MSCs onto scaffolds frequently results in a significant loss of cells and the random dispersal of cells in the biological scaffold frequently leads to inefficient or inadequate bone regeneration, cell sheet technology was developed as a promising approach to solve these problems (2). This avoids applying trypsin and EDTA to improve the utilization of MSCs to the utmost and prevents degradation of cell-surface proteins and the ECM, which is responsible for transmitting biological signals to regulate biological activity and bone formation (24). In addition, growth factors secreted by stem cells may be preserved for a longer period of time in the ECM, suggesting that the cell sheet may act as a controlled release system (25). Several studies have demonstrated that through the ECM, stem cells

may exert therapeutic effects via the secretion of trophic factors that provide a favorable microenvironment for cell survival, renewal and differentiation, ultimately having a positive role in bone regeneration (26). Furthermore, cell sheets always contract when harvested from culture dishes and shrinkage-generated stress has been considered to specifically regulate the polarization of MSCs and activate their differentiation as a biomechanical force (27). In recent years, cell sheet-based tissue engineering technology has already been applied for treating various soft-tissue defects, such as the cornea, myocardium and periodontal ligament (28). This has also been progressively popular for hard-tissue engineering, including bone tissues. Furthermore, it has been reported that MSC sheets have a higher capacity of bone regeneration and reconstruction for healing bone defects compared to scattered MSCs, both *in vitro* and *in vivo* (2,25). Consistent with the previous literature, the ADSC sheet in the present study exhibited better osteogenic ability with enhanced ALP activity, more calcium deposition and an elevated expression level of OCN and OPN when compared to suspended ADSCs.

A number of approaches to harvesting intact cell sheets have been previously reported, including temperature-responsive culture (29), magnetic force (30), electron beam irradiation (31) and vitamin C application (32). However, these mentioned approaches require complex procedures and novel materials, which may affect cell proliferation or differentiation. In the present study, the ADSC cell sheets were comprised of multiple layers of osteoprogenitor cells and endogenous ECMs. With the large amount of ECM and its gradual mineralization, the sheets were sufficiently robust to be detached while remaining intact with a scraper and forceps, making it possible to wrap it over the β-TCP/COL-I and form a 3D compound. In addition, the present procedures are simple and practical with the common tissue culture dish and cell scraper.

Although a series of studies reported on harvesting an osteogenic cell sheet and using it for bone reconstruction without any scaffold (33), these scaffold-free cell sheets were unsuitable for large bone defects due to poor mechanical properties at the early stage of healing (34). Even for multilayer cell sheets, manual operation should be performed with care to prevent the cell sheet from being torn. The biomaterial scaffold may provide a 3D structure for the seeding cells to form a composite with a certain shape and this may be transplanted into large bone defects (35). Bone tissue engineering requires scaffolds with appropriate architecture and good osteoconductive activity, including the following (12,36): i) An appropriate pore size within 50-100 μm; ii) interconnected porosity for living tissues to grow; iii) sufficient mechanical properties; iv) controllable degradation efficiency; v) excellent biocompatibility; and vi) low immunogenicity. Mixtures of organic and inorganic materials have been frequently used to tackle those drawbacks of single materials and achieve the optimum desired physical and chemical properties (37). The inorganic β-TCP has a relative high biodegradability and osteoconductivity in comparison with other materials like nano-hydroxyapatite/polymer or polymer-calcium phosphate cement (17). And the organic collagen is a major component of bone and has good cell attachment ability and profound biodegradability (17). They are the commonly used bone substitute materials that meet bone tissue engineering requirements to the utmost extent. In addition, β-TCP was proven suitable as an osteogenic material to repair bone in an animal model, as well as in a clinical setting (38). While the mechanical properties of pure collagen (37) or β-TCP (38) are frequently poor, the β-TCP/COL-I scaffold had a higher compressive modulus (16), which is highly affected by the material degradation and ECM formation under *in vitro* culture conditions (14). Arahira and Todo (39) reported that the compressive modulus and strength of the β-TCP/COL scaffold with rat bone-marrow mesenchymal stem cells (rBMSCs) decreased due to the local release of β-TCP particles during the early culture period and then increased as ECM deposition occurred in the late stage, and finally became higher than those of the β-TCP/COL scaffold without rBMSCs, which remained constant for the whole experiment. The previous study by our group demonstrated that β-TCP/COL-I scaffolds were able to enhance the bone regeneration potential of rBMSC sheets *in vitro* and *in vivo* (10). In the present study, bone-like collagen fibrils integrated with homogeneous β-TCP particles were used as units to construct the β-TCP/COL-I scaffold in order to mimic the constituent and structural properties of natural bone. The porous structure of this composite facilitates the attachment and ingrowth of local cells (37) and provides a sufficient supply of nutrients and oxygen due to the neovascularization (17,40). The present study indicated that the ADSCs were able to tightly adhere and grow on the surface of the β-TCP/COL-I scaffold without any impairment of cell viability compared to ADSCs only, indicating that this material had good biocompatibility. Furthermore, ADSC sheets wrapped around a β-TCP/COL-I scaffold expressed higher levels of ALP, OCN and OPN when compared to a mere ADSC sheet, suggesting that the scaffold was able to significantly enhance the osteogenic activity of the ADSC sheet, rather than just providing structural support. The possible mechanism is that the mechanical properties of the scaffold may help the ADSC sheet to resist the inherent retraction tendency of the cell sheet, which is unfavorable for cell proliferation and differentiation.

The present study provided a basic and novel approach for bone engineering. Further studies should focus on the development of new materials, alone or with bioactive factors (41-44) to enhance the osteogenic capacity of ADSC sheets. In addition, various preparation methods should be tested to make the composition, morphology and mechanical properties of the scaffold closer to natural bone, and improve the practicability of the use of ADSC sheets in regenerating bone tissues (45,46).

There are two shortcomings of the current study, which may be addressed in the future. ADSCs should be comprehensively compared with other MSCs, including rBMSCs, in terms of osteoconductive activity when combined with a β-TCP/COL-I scaffold *in vitro* and *in vivo*, to determine which is more effective in bone engineering. In addition, the mechanical properties of the β-TCP/COL-I scaffold with and without ADSCs should be tested to prove their durability.

In conclusion, the present study demonstrated that ADSC sheets combined with a β-TCP/COL-I scaffold have more substantial osteogenic potential when compared to scattered ADSCs with a β-TCP/COL-I scaffold or an ADSC sheet alone. The synergistic effect of the ECM in the cell sheet and the mechanical properties of the scaffold may have a vital role in the improved osteogenic potential. The combination of the

ADSC sheet and β-TCP/COL-I scaffold provides an advanced strategy for treating bone defects, which may be used to enhance treatment outcomes in the future.

Acknowledgements

Not applicable.

Funding

The present study was supported by two projects from the National Natural Science Foundation of China (grant nos. 81873937 and 81970978).

Availability of data and materials

The datasets used and/or analyzed during the present study are available from the corresponding author on reasonable request.

Authors' contributions

JX designed all of the experiments. YW wrote the manuscript. YW, XJS, RL, NZ and LZ performed the experiments. WX and JL analyzed the data. YW and JX checked and confirmed the authenticity of the raw data. All authors have discussed the data and commented on the manuscript. All the authors have read and approved the final version of this manuscript.

Ethics approval and consent to participate

All animal experiments and the protocol of the present study were conducted according to the guidelines of the Ethics Committee of the Laboratory Animal Center, the First Affiliated Hospital, School of Medicine, Zhejiang University (Hangzhou, China).

Patient consent for publication

Not applicable.

Competing interests

The authors declare that they have no competing interests.

References

1. Han Y, Li X, Zhang Y, Han Y, Chang F and Ding J: Mesenchymal stem cells for regenerative medicine. Cells 8: 886, 2019.
2. Xu X, Fang K, Wang L, Liu X, Zhou Y and Song Y: Local application of semaphorin 3A combined with adipose-derived stem cell sheet and anorganic bovine bone granules enhances bone regeneration in type 2 diabetes mellitus rats. Stem Cells Int 2019: 2506463, 2019.
3. Jin HJ, Bae YK, Kim M, Kwon S-J, Jeon HB, Choi SJ, Kim SW, Yang YS, Oh W and Chang JW: Comparative analysis of human mesenchymal stem cells from bone marrow, adipose tissue, and umbilical cord blood as sources of cell therapy. Int J Mol Sci 14: 17986-18001, 2013.
4. Mazini L, Rochette L, Amine M and Malka G: Regenerative capacity of adipose derived stem cells (ADSCs), comparison with mesenchymal stem cells (MSCs). Int J Mol Sci 20: E2523, 2019.
5. Ebrahimian TG, Pouzoulet F, Squiban C, Buard V, André M, Cousin B, Gourmelon P, Benderitter M, Casteilla L and Tamarat R: Cell therapy based on adipose tissue-derived stromal cells promotes physiological and pathological wound healing. Arterioscler Thromb Vasc Biol 29: 503-510, 2009.
6. Li M, Ma J, Gao Y and Yang L: Cell sheet technology: A promising strategy in regenerative medicine. Cytotherapy 21: 3-16, 2019.
7. Chen M, Xu Y, Zhang T, Ma Y, Liu J, Yuan B, Chen X, Zhou P, Zhao X, Pang F, *et al*: Mesenchymal stem cell sheets: A new cell-based strategy for bone repair and regeneration. Biotechnol Lett 41: 305-318, 2019.
8. Maruthamuthu V, Sabass B, Schwarz US and Gardel ML: Cell-ECM traction force modulates endogenous tension at cell-cell contacts. Proc Natl Acad Sci USA 108: 4708-4713, 2011.
9. Sasagawa T, Shimizu T, Sekiya S, Haraguchi Y, Yamato M, Sawa Y and Okano T: Design of prevascularized three-dimensional cell-dense tissues using a cell sheet stacking manipulation technology. Biomaterials 31: 1646-1654, 2010.
10. Lin J, Shao J, Juan L, Yu W, Song X, Liu P, Weng W, Xu J and Mehl C: Enhancing bone regeneration by combining mesenchymal stem cell sheets with β-TCP/COL-I scaffolds. J Biomed Mater Res B Appl Biomater 106: 2037-2045, 2018.
11. Hutmacher DW, Schantz JT, Lam CX, Tan KC and Lim TC: State of the art and future directions of scaffold-based bone engineering from a biomaterials perspective. J Tissue Eng Regen Med 1: 245-260, 2007.
12. Zhu T, Cui Y, Zhang M, Zhao D, Liu G and Ding J: Engineered three-dimensional scaffolds for enhanced bone regeneration in osteonecrosis. Bioact Mater 5: 584-601, 2020.
13. Pereira HF, Cengiz IF, Silva FS, Reis RL and Oliveira JM: Scaffolds and coatings for bone regeneration. J Mater Sci Mater Med 31: 27, 2020.
14. Arahira T and Todo M: Effects of proliferation and differentiation of mesenchymal stem cells on compressive mechanical behavior of collagen/β-TCP composite scaffold. J Mech Behav Biomed Mater 39: 218-230, 2014.
15. Kang Y, Kim S, Bishop J, Khademhosseini A and Yang Y: The osteogenic differentiation of human bone marrow MSCs on HUVEC-derived ECM and β-TCP scaffold. Biomaterials 33: 6998-7007, 2012.
16. Baheiraei N, Nourani MR, Mortazavi SMJ, Movahedin M, Eyni H, Bagheri F and Norahan MH: Development of a bioactive porous collagen/β-tricalcium phosphate bone graft assisting rapid vascularization for bone tissue engineering applications. J Biomed Mater Res A 106: 73-85, 2018.
17. Zou C, Weng W, Deng X, Cheng K, Liu X, Du P, Shen G and Han G: Preparation and characterization of porous beta-tricalcium phosphate/collagen composites with an integrated structure. Biomaterials 26: 5276-5284, 2005.
18. Li JJ, Akey A, Dunstan CR, Vielreicher M, Friedrich O, Bell DC and Zreiqat H: Effects of material-tissue interactions on bone regeneration outcomes using baghdadite implants in a large animal model. Adv Healthc Mater 7: e1800218, 2018.
19. Wubneh A, Tsekoura EK, Ayranci C and Uludağ H: Current state of fabrication technologies and materials for bone tissue engineering. Acta Biomater 80: 1-30, 2018.
20. Birmingham E, Niebur GL, McHugh PE, Shaw G, Barry FP and McNamara LM: Osteogenic differentiation of mesenchymal stem cells is regulated by osteocyte and osteoblast cells in a simplified bone niche. Eur Cell Mater 23: 13-27, 2012.
21. Wu V, Helder MN, Bravenboer N, Ten Bruggenkate CM, Jin J, Klein-Nulend J and Schulten EAJM: Bone tissue regeneration in the oral and maxillofacial region: a review on the application of stem cells and new strategies to improve vascularization. Stem Cells Int 2019: 6279721, 2019.
22. Tropel P, Noël D, Platet N, Legrand P, Benabid A-L and Berger F: Isolation and characterisation of mesenchymal stem cells from adult mouse bone marrow. Exp Cell Res 295: 395-406, 2004.
23. Si Z, Wang X, Sun C, Kang Y, Xu J, Wang X and Hui Y: Adipose-derived stem cells: Sources, potency, and implications for regenerative therapies. Biomed Pharmacother 114: 108765, 2019.
24. Martino MM, Mochizuki M, Rothenfluh DA, Rempel SA, Hubbell JA and Barker TH: Controlling integrin specificity and stem cell differentiation in 2D and 3D environments through regulation of fibronectin domain stability. Biomaterials 30: 1089-1097, 2009.
25. Liu Y, Ming L, Luo H, Liu W, Zhang Y, Liu H and Jin Y: Integration of a calcined bovine bone and BMSC-sheet 3D scaffold and the promotion of bone regeneration in large defects. Biomaterials 34: 9998-10006, 2013.
26. Pensak M, Hong S, Dukas A, Tinsley B, Drissi H, Tang A, Cote M, Sugiyama O, Lichtler A, Rowe D, *et al*: The role of transduced bone marrow cells overexpressing BMP-2 in healing critical-sized defects in a mouse femur. Gene Ther 22: 467-475, 2015.

27. Yang J, Yamato M, Nishida K, Ohki T, Kanzaki M, Sekine H, Shimizu T and Okano T: Cell delivery in regenerative medicine: The cell sheet engineering approach. J Control Release 116: 193-203, 2006.
28. Hasegawa M, Yamato M, Kikuchi A, Okano T and Ishikawa I: Human periodontal ligament cell sheets can regenerate periodontal ligament tissue in an athymic rat model. Tissue Eng 11: 469-478, 2005.
29. Okano T, Yamada N, Sakai H and Sakurai Y: A novel recovery system for cultured cells using plasma-treated polystyrene dishes grafted with poly(N-isopropylacrylamide). J Biomed Mater Res 27: 1243-1251, 1993.
30. Penland N, Choi E, Perla M, Park J and Kim DH: Facile fabrication of tissue-engineered constructs using nanopatterned cell sheets and magnetic levitation. Nanotechnology 28: 075103, 2017.
31. Kwon OH, Kikuchi A, Yamato M, Sakurai Y and Okano T: Rapid cell sheet detachment from poly(N-isopropylacrylamide)-grafted porous cell culture membranes. J Biomed Mater Res 50: 82-89, 2000.
32. Nakamura A, Akahane M, Shigematsu H, Tadokoro M, Morita Y, Ohgushi H, Dohi Y, Imamura T and Tanaka Y: Cell sheet transplantation of cultured mesenchymal stem cells enhances bone formation in a rat nonunion model. Bone 46: 418-424, 2010.
33. Ma D, Ren L, Liu Y, Chen F, Zhang J, Xue Z and Mao T: Engineering scaffold-free bone tissue using bone marrow stromal cell sheets. J Orthop Res 28: 697-702, 2010.
34. Ma D, Yao H, Tian W, Chen F, Liu Y, Mao T and Ren L: Enhancing bone formation by transplantation of a scaffold-free tissue-engineered periosteum in a rabbit model. Clin Oral Implants Res 22: 1193-1199, 2011.
35. Yuan J, Cui L, Zhang WJ, Liu W and Cao Y: Repair of canine mandibular bone defects with bone marrow stromal cells and porous beta-tricalcium phosphate. Biomaterials 28: 1005-1013, 2007.
36. Li X, Wang L, Fan Y, Feng Q, Cui FZ and Watari F: Nanostructured scaffolds for bone tissue engineering. J Biomed Mater Res A 101: 2424-2435, 2013.
37. Zhang Y, Liu X, Zeng L, Zhang J, Zuo J, Zou J, Ding J and Chen X: Polymer Fiber Scaffolds for Bone and Cartilage Tissue Engineering. Adv Funct Mater 29: 1903279, 2019.
38. Luvizuto ER, Queiroz TP, Margonar R, Panzarini SR, Hochuli-Vieira E, Okamoto T and Okamoto R: Osteoconductive properties of β-tricalcium phosphate matrix, polylactic and polyglycolic acid gel, and calcium phosphate cement in bone defects. J Craniofac Surg 23: e430-e433, 2012.
39. Arahira T and Todo M: Variation of mechanical behavior of β-TCP/collagen two phase composite scaffold with mesenchymal stem cell in vitro. J Mech Behav Biomed Mater 61: 464-474, 2016.
40. Zhou Y, Chen F, Ho ST, Woodruff MA, Lim TM and Hutmacher DW: Combined marrow stromal cell-sheet techniques and high-strength biodegradable composite scaffolds for engineered functional bone grafts. Biomaterials 28: 814-824, 2007.
41. Zhang Y, Ding J, Qi B, Tao W, Wang J, Zhao C, Peng H and Shi J: Multifunctional fibers to shape future biomedical devices. Adv Funct Mater 29: 1902834, 2019.
42. Cui L, Zhang J, Zou J, Yang X, Guo H, Tian H, Zhang P, Wang Y, Zhang N, Zhuang X, *et al*: Electroactive composite scaffold with locally expressed osteoinductive factor for synergistic bone repair upon electrical stimulation. Biomaterials 230: 119617, 2020.
43. Qiu H, Guo H, Li D, Hou Y, Kuang T and Ding J: Intravesical hydrogels as drug reservoirs. Trends Biotechnol 38: 579-583, 2020.
44. Wang Y, Jiang Z, Xu W, Yang Y, Zhuang X, Ding J and Chen X: Chiral polypeptide thermogels induce controlled inflammatory response as potential immunoadjuvants. ACS Appl Mater Interfaces 11: 8725-8730, 2019.
45. Ding J, Xiao H, Li J, Zhuang X, Zhang J, Di Li XC, Xiao C and Yang H: Electrospun polymer biomaterials. Prog Polym Sci 90: 1-34, 2019.
46. Feng X, Li J, Zhang X, Liu T, Ding J and Chen X: Electrospun polymer micro/nanofibers as pharmaceutical repositories for healthcare. J Control Release 302: 19-41, 2019.